Full-Wafer Characterization of AlGaN/GaN HEMTs on Free-Standing CVD Diamond Substrates

Kelson D. Chabak, James K. Gillespie, *Member, IEEE*, Virginia Miller, Antonio Crespo, Jason Roussos, Manuel Trejo, *Student Member, IEEE*, Dennis E. Walker, Jr., Glen D. Via, Gregg H. Jessen, *Senior Member, IEEE*, John Wasserbauer, Firooz Faili, *Member, IEEE*, Dubravko I. Babić, *Member, IEEE*, Daniel Francis, and Felix Ejeckam

***Abstract*—We report on electrical characterization and uniformity measurements of the first conventionally processed AlGaN/GaN high electron mobility transistors (HEMTs) on free-standing chemical-vapor-deposited (CVD) diamond substrate wafers. DC and RF device performance is reported on HEMTs fabricated on ∼130-μm-thick and 30-mm round CVD diamond substrates without mechanical carrying wafers. A measured $f_T \cdot L_G$ product of 12.5 GHz $\cdot$ μm is the best reported data for all GaN-on-diamond technology. X-band power performance of AlGaN/GaN HEMTs on diamond is reported to be 2.08 W/mm and 44.1% power added efficiency. This letter demonstrates the potential for GaN HEMTs to be fabricated on CVD diamond substrates utilizing contact lithography process techniques. Further optimization of the epitaxy and diamond substrate attachment process could provide for improvements in thermal spreading while preserving the electrical properties.**

***Index Terms*—Chemical vapor deposited (CVD) diamond substrate, GaN-on-diamond, high electron mobility transistor (HEMT).**

I. INTRODUCTION

AlGaN/GaN high electron mobility transistors (HEMTs) are actively pursued for high-speed and high-power applications [1]. Impressive sheet charge density and breakdown voltage characteristics of AlGaN/GaN devices have enabled high-output-power operation exceeding 30–40 W/mm [2], [3]. However, notable thermal management consequences are inevitable at such high power levels. Reliability concerns resulting from localized device heating have been reported even on high thermal conducting SiC substrates at high drain voltage bias [4]. As a solution, attempts to use chemical-vapor-deposited (CVD) diamond substrates for AlGaN/GaN HEMTs have shown some promise [5]–[9]. Diamond has a remarkable thermal conductivity coefficient of 1200 W/m/K—approximately three times that of SiC [10]. Furthermore, growing polycrystalline diamond by CVD technique is considerably cheaper than SiC.

Challenges to integrate diamond substrates into conventional semiconductor processing techniques have evolved over the past few years. SP3 Labs reported silicon-on-diamond thermal spreading technology where 1 to 50 μm of CVD diamond is located 2 to 4 μm beneath the AlGaN/GaN device active layer [8]. The mechanical support for this wafer is an integrated polysilicon wafer. This part of the substrate is required to be removed once processing is complete. Group4 Labs developed a similar process where the AlGaN/GaN active layers are grown on Si (111) substrate and atomically attached to a 25-μm-thick CVD diamond substrate [5]–[7]. The CVD diamond is located approximately 1.2 μm below the active layer, and a mechanical carrier wafer is required for HEMT fabrication. In both technologies, the diamond was less than 50-μm thick. In this letter, we report on dc/RF device measurements across two 30-mm round CVD diamond substrates. X-band power measurements are also presented from these devices.

II. FABRICATION AND MEASUREMENTS

HEMT devices were grown on Si (111) substrates by metal organic chemical vapor deposition (MOCVD). An AlN nucleation layer was grown first followed by a 0.8-μm GaN buffer layer and 175-Å $Al_{0.26}Ga_{0.74}N$ barrier layer. A 20-Å GaN cap layer was also grown to effectively enhance the Schottky barrier height [11]. Following MOCVD growth, 230 nm of SiN was deposited on the cap layer to protect the epitaxy during the transfer process. The wafer was front-side mounted to a mechanical wafer, and the silicon substrate was removed. Subsequently, the 130-μm CVD diamond substrate was atomically attached to the GaN buffer layer using a Group4 Labs proprietary process.

AlGaN/GaN HEMT devices were fabricated using standard Air Force Research Laboratory contact lithography on two 30-mm round CVD diamond substrates. Mesa isolation was performed using a two-step $BCl_3/Cl_2/Ar$ and Cl_2/Ar recipe in a PlasmaTherm 770 ICP system. A Ti/Al/Ni/Au ohmic metal stack was evaporated and annealed in a nitrogen environment at 850 °C for 30 s. The source–drain spacing of all measured devices is ∼4.5 μm. Two-finger Ni/Au gates were deposited with

Manuscript received October 6, 2009; revised October 28, 2009. First published December 15, 2009; current version published January 27, 2010. The review of this letter was arranged by Editor G. Meneghesso.

K. D. Chabak, J. K. Gillespie, V. Miller, A. Crespo, M. Trejo, G. D. Via, and G. H. Jessen are with the Air Force Research Laboratory, Sensors Directorate, Wright-Patterson Air Force Base, Dayton, OH 45433 USA (e-mail: kelson.chabak@us.af.mil; james.gillespie@wpafb.af.mil; virginia.miller@wpafb.af.mil; antonio.crespo@wpafb.af.mil; manuel.trejo@wpafb.af.mil; glen.via@wpafb.af.mil; gregg.jessen@aoard.af.mil).

J. Roussos is with the Naval Research Laboratory, Washington, DC 20375 USA (e-mail: roussos@nrl.navy.mil).

D. E. Walker, Jr. is with the Air Force Research Laboratory, Sensors Directorate, Wright-Patterson Air Force Base, Dayton, OH 45433 USA and also with Wyle Laboratories, Dayton, OH 45431 USA (e-mail: dennis.walker@wpafb.af.mil).

J. Wasserbauer, F. Faili, D. I. Babić, D. Francis, and F. Ejeckam are with the Group 4 Labs, LLC, Menlo Park, CA 95025 USA (e-mail: john_wasserbauer@group4labs.com; firooz_faili@group4labs.com; dubravko_babic@group4labs.com; daniel_francis@group4labs.com; felix_ejeckam@group4labs.com).

Color versions of one or more of the figures in this letter are available online at http://ieeexplore.ieee.org.

Digital Object Identifier 10.1109/LED.2009.2036574

0741-3106/$26.00 © 2009 IEEE

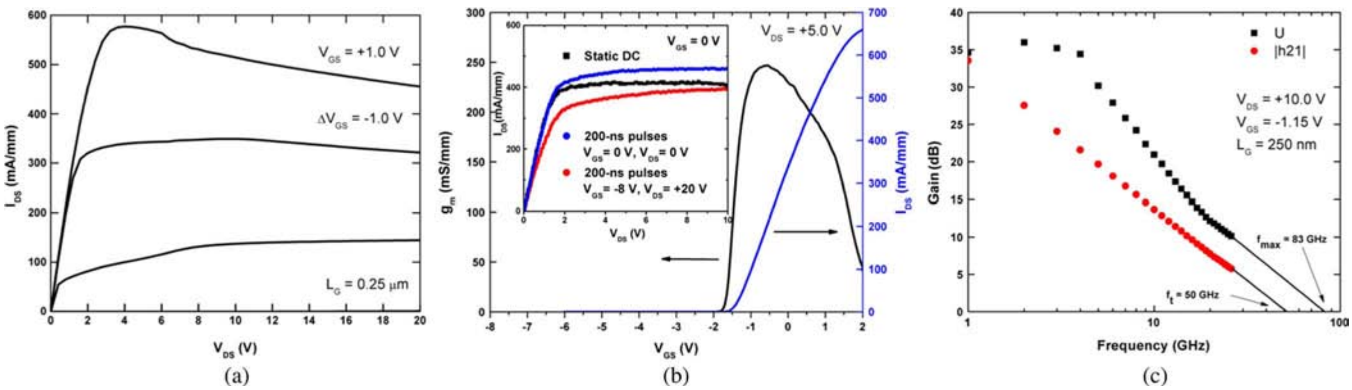

Fig. 1. (a) DC current-voltage measurements. (b) Transfer characteristics of an AlGaN/GaN-on-diamond HEMT device with $2 \times 150\,\mu$m $\times$ $0.25\,\mu$m gate periphery, also showing (inset) the 200-ns pulsed and static dc current–voltage measurements at $V_{\rm GS} = 0$ V. (c) Corresponding frequency response measured at $V_{\rm DS} = +10$ V, showing performance of $f_t/f_{\max}$ = 50/83 GHz.

gate length and gate width dimensions of 250 nm and 150 μm for each finger, respectively. The 250-nm T-gate process used a JEOL6300 direct write E-beam system. The devices were passivated with 100-nm PECVD Si_3N_4 deposited at 300 °C.

DC and RF characterization was performed on process control monitor (PCM) structures and e-beam-defined transistors across the whole wafer. PCM structures were measured on a Keithley 450, and dc device data were taken with an HP4142 with bias tees and Cascade Microtech probes. Small signal s-parameters were measured from 1 to 26 GHz with an HP8510 vector-network analyzer and the same on-wafer probes. Power measurements were obtained under prematched continuous wave (CW) class A operation for maximum power added efficiency (PAE) at a 10-GHz X-band. The wafer was conventionally cooled on the chuck and held in place by vacuum during all characterization.

III. Results and Discussion

Transmission line measurement structures were used to obtain ohmic contact resistance (R_c) and material sheet resistance $(R_{\rm sh})$ values of $0.34 \pm 0.16\ \Omega \cdot$ mm and $638.0 \pm 25.0\ \Omega$/sq, respectively. Room temperature Hall effect mobility tests using passivated on-wafer van der Pauw structures measured a carrier mobility of $\sim$1180 cm^2/V $\cdot$ s and sheet charge density of $\sim 9.5 \times 10^{12}$ cm^{-2}. Mesa isolation structures were used to verify the insulating GaN buffer. An average of $0.47 \pm 0.14\ \mu$A was measured at 50 V for 5-μm mesa gap structures for all fabricated reticles.

Fig. 1 shows the representative dc I–V characterization performed on individual sites. The family of I–V curves is shown in Fig. 1(a), with the gate-source voltage stepped from $+1.0$ to -3.0 V in -1.0-V increments, and the drain-source voltage is swept to $+20.0$ V. The knee voltage at $V_{\rm GS} = 0$ V is $+1.52$ V, which is markedly lower than our previous work in [6] owing to a decreased ohmic contact resistance. The low $I_{\rm DS,sat}$ is attributed to the high $R_{\rm sh}$ resulting from both the unoptimized epitaxial and CVD diamond layers. We expect the drain current at the forward bias gate voltages to improve with thicker CVD diamond substrates and future packaged HEMT devices. Fig. 1(b) shows a peak transconductance of 247 mS/mm, observed at $V_{\rm GS} = -0.55$ V and $V_{\rm DS} = +5.0$ V for the same device. The device exhibited good on/off properties with a threshold voltage (V_T) of -1.4 V. The inset graph shows the representative 200-ns pulsed I–V characteristics at the $V_{\rm GS} = 0$ V condition from quiescent points of $V_{\rm GS} = -8.0$ V and $V_{\rm DS} = +20.0$ V, and $V_{\rm GS} = 0$ V and $V_{\rm DS} = 0$ V.

Fig. 1(c) shows the $|h_{21}|$ and Mason's unilateral power gain (U) from measured s-parameters at $V_{\rm GS} = -1.15$ V and $V_{\rm DS} = +10.0$ V. The unity current gain cutoff frequency (f_T) and power gain cutoff frequency $(f_{\max,U})$ was 50 and 83 GHz, respectively. The $f_T \cdot L_G$ product is approximately 12.5 GHz $\cdot\ \mu$m, which fits well to the model proposed by Jessen *et al.*, given our $L_G/t_{\rm bar}$ ratio of 14.3, indicating minimal short-channel effects [13]. For this particular geometry, the $f_T \cdot L_G$ product shown here is the best reported one for all GaN-on-diamond fabricated devices.

Representative large signal power results measured at X-band are shown in Fig. 2(a). The input power was swept from approximately -5 to 15 dB. A maximum PAE of 44.1% was measured at $V_{\rm DS} = +25.0$ V and $V_{\rm GS} = -1.2$ V. The gain was 14.6 dB at the same input power. Additional parameters include a maximum output power and gain of 2.08 W/mm and 20.3 dB, respectively, for $V_{\rm DS} = +30.0$ V and $V_{\rm GS} = -1.1$ V. The low output power and moderate PAE is most likely a result of the high $R_{\rm sh}$ and thermal degradation. To our knowledge, this is the first report of power measurements made on free-standing CVD diamond substrates.

Automated dc and RF characterization was also performed on all wafer reticles to study uniformity. Example wafer maps are shown in Fig. 2(b). Additional full-wafer device results are displayed in Table I. These results show the first demonstration of dc and RF device performance measurements on free-standing CVD diamond substrates.

IV. Conclusion

We have demonstrated and are the first to report on full-wafer electrical characterization of AlGaN/GaN HEMTs on free-standing CVD diamond substrates. On-wafer uniformity measurements of PCM and AlGaN/GaN HEMT devices were shown. DC/RF and power measurements demonstrated typical AlGaN/GaN device performance for devices with $R_{\rm sh} \sim$ 640 Ω/sq using CVD diamond as the substrate material. More research is planned to improve the uniformity of the device metrics, optimize the material structure (epitaxial layers,

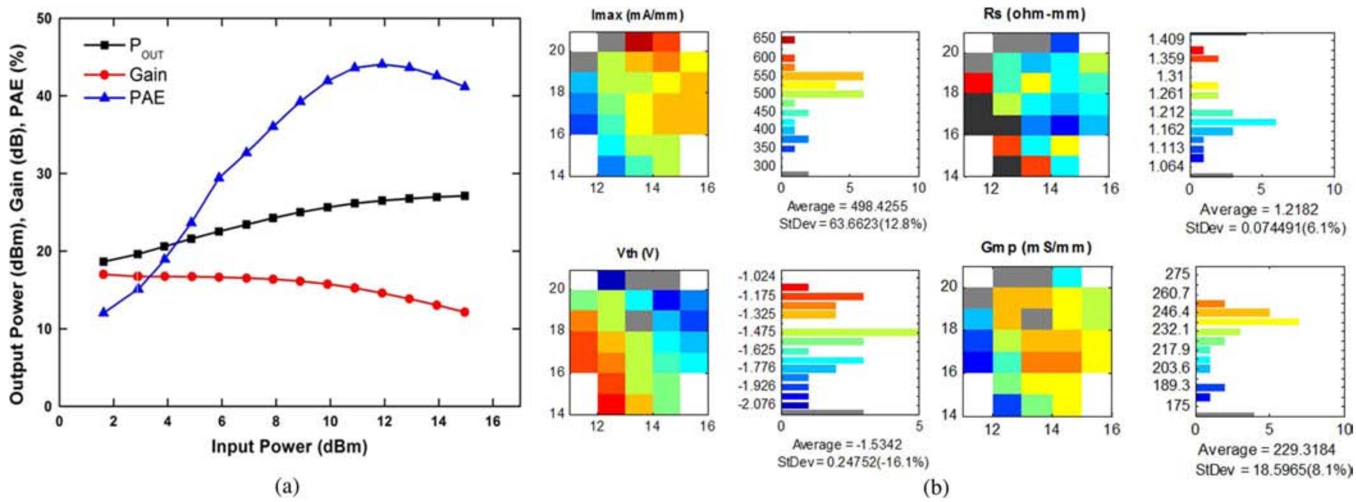

Fig. 2. (a) X-band 10-GHz CW power characteristics of an AlGaN/GaN-on-diamond HEMT with $2 \times 150\ \mu$m $\times$ $0.25\ \mu$m gate periphery, showing a peak PAE of 44.1% and a 14.6-dB gain at 11.9-dB input power for $V_{\rm DS} = +25$ V. (b) Wafer maps of $I_{\rm DS,max}$, V_T, R_S, and $g_{m,\rm peak}$ with corresponding histograms showing the uniformity of dc/RF performance over the 30-mm CVD diamond substrate.

TABLE I
FULL-WAFER DEVICE PARAMETER MEASUREMENTS

Parameter	Average Value	Std. Deviation
R_C	0.34 Ω·mm	± 0.11 Ω·mm (31.4%)
R_{sh}	637.9 Ω/sq	± 25.0 Ω/sq (3.9%)
R_S	1.22 Ω·mm	± 0.07 Ω·mm (6.1%)
$I_{DS,max}$	498.4 mA/mm	± 63.7 mA/mm (12.8%)
$g_{m,peak}$	229.3 mS/mm	± 18.6 mS/mm (8.1%)
C_{gs}	955.1 fF/mm	± 81.5 fF/mm (8.5%)
V_T	-1.53 V	± 0.25 V (16.1%)
V_{BR}[a]	47.9 V	± 4.1 V (8.7%)
f_t	47.9 GHz	± 3.2 GHz (6.7%)
$f_{max,U}$	83.9 GHz	± 1.9 GHz (2.3%)

[a]Breakdown voltage measured at I_{DS}=1 mA/mm and $V_{GS} < V_T$.

CVD diamond material, and bonding interface), and show that this material structure is superior to conventional GaN-on-SiC technology.

ACKNOWLEDGMENT

The authors would like to thank J. Breedlove, P. Cassity, and T. Cooper for the assistance with metal depositions, etching, and Hall measurements; the Navy Research Laboratory for the assistance with power measurements; and Group4 Labs for supplying the CVD diamond substrates.

REFERENCES

[1] U. K. Mishra, L. Shen, T. E. Kazior, and Y.-F. Wu, "GaN based RF power devices and amplifiers," *Proc. IEEE*, vol. 96, no. 2, pp. 287–305, Feb. 2008.

[2] Y.-F. Wu, A. Saxler, M. Moore, P. Smith, S. Sheppard, M. Chavarkar, T. Wisleder, K. Mishra, and P. Parikh, "30-W/mm GaN HEMTs by field plate optimization," *IEEE Electron Device Lett.*, vol. 25, no. 3, pp. 117–119, Mar. 2004.

[3] Y. F. Wu, M. Moore, A. Saxler, T. Wisleder, and P. Parikh, "40-W/mm double field-plated GaN HEMTs," in *Proc. IEEE DRC Conf. Dig.*, 2006, pp. 151–152.

[4] Y. C. Chou, D. Leung, I. Smorchkova, M. Wojtowicz, R. Grundbacher, L. Callejo, Q. Kan, R. Lai, P. H. Liu, D. Eng, and A. Oki, "Degradation of AlGaN/GaN HEMTs under elevated temperature life testing," *Microelectron. Reliab.*, vol. 44, no. 7, pp. 1033–1038, Jul. 2004.

[5] D. C. Dumka and P. Saunier, "AlGaN/GaN HEMTs on diamond substrate," in *Proc. IEEE DRC Conf. Dig*, 2007, pp. 31–32.

[6] G. H. Jessen, J. K. Gillespie, G. D. Via, A. Crespo, D. Langley, J. Wasserbauer, F. Faili, D. Francis, D. Babic, F. Ejeckam, S. Guo, and I. Eliashevich, "AlGaN/GaN HEMT on diamond technology demonstration," in *Proc. IEEE Compound Semicond. Ingter. Circuit Symp. Tech. Dig.*, 2006, pp. 271–274.

[7] J. G. Felbinger, M. V. S. Chandra, Y. Sun, L. F. Lester, J. Wasserbauer, F. Faili, D. Babic, D. Francis, and F. Ejeckman, "Comparison of GaN HEMTs on diamond and SiC substrates," *IEEE Electron Device Lett.*, vol. 28, no. 11, pp. 948–950, Nov. 2007.

[8] J. W. Zimmer and G. Chandler, "Advances in large diameter GaN on diamond substrates," in *Proc. CS MANTECH*, Chicago, IL, Apr. 14–17, 2008.

[9] Q. Diduck, J. Felbinger, L. F. Eastman, D. Francis, J. Wasserbauer, F. Faili, D. I. Babic, and F. Ejeckam, "Frequency performance enhancement of AlGaN/GaN HEMTs on diamond," *Electron. Lett.*, vol. 45, no. 14, pp. 758–759, Jul. 2009.

[10] J. Calame, R. Myers, F. Wood, and S. Binari, "Simulations of direct-die-attached microchannel coolers for the thermal management of GaN-on-SiC microwave amplifiers," *IEEE Trans. Compon. Packag. Technol.*, vol. 28, no. 4, pp. 797–809, Dec. 2005.

[11] E. T. Yu, X. Z. Dang, L. S. Yu, D. Qiao, P. M. Asbeck, S. S. Lau, G. J. Sullivan, K. S. Boutros, and J. M. Redwing, "Schottky barrier engineering in III–V nitrides via the piezoelectric effect," *Appl. Phys. Lett.*, vol. 73, no. 13, pp. 1880–1882, Sep. 1998.

[12] D. H. Kim, V. Kumar, G. Chen, A. M. Dabiran, A. M. Wowchak, A. Osinsky, and I. Adesida, "ALD Al_2O_3 passivated MBE-grown AlGaN/GaN HEMTs on 6H-SiC," *Electron. Lett.*, vol. 43, no. 2, pp. 129–130, Jan. 2007.

[13] G. H. Jessen, R. C. Fitch, J. K. Gillespie, G. Via, A. Crespo, D. Langley, D. J. Denninghoff, M. Trejo, and E. R. Heller, "Short-channel effect limitations on high-frequency operation of AlGaN/GaN HEMTs for T-gate devices," *IEEE Trans. Electron Devices*, vol. 54, no. 10, pp. 2589–2597, Oct. 2007.